

QUANTITATIVE CONTROL OF OPTICAL CLEARING EFFECTS STUDIED WITH TISSUE-LIKE PHANTOM

JINGYING JIANG^{*,†}, WEI CHEN^{*}, QILIANG GONG^{*} and KEXIN XU[†]

^{*}Department of Biomedical Engineering, College of Precision
Instruments and Opto-Electronics Engineering, Tianjin University
Tianjin 300072, China

[†]State Key Laboratory of Precision Measuring Technology and Instruments
Tianjin University, Tianjin 300072, China

[‡]jingying@tju.edu.cn

Tissue optical clearing by use of optical clearing agents (OCAs) has been proven to have potential to reduce the highly scattering effect of biological tissues in optical techniques. However, the difference in tissue samples could lead to unreliable results, making it difficult to quantitatively control the dose of OCAs during the course of tissue optical clearing. In this work, in order to study the effects of optical clearing, we customized tissue-like phantoms with optical properties of some biological tissue. Diffuse reflectance and total transmittance of tissue-like phantoms with different OCAs (DMSO or glycerol) and porcine skin tissues were measured. Then optical property parameters were calculated by inverse adding-doubling (IAD) algorithm. Results showed that OCAs could lead to a reduction in scattering of tissue-like phantoms as it did to porcine skin tissue *in vitro*. Furthermore, a series of relational expressions could be fit to quantitatively describe the relationship between the doses of OCAs and the reduction of scattering effects. Therefore, proper tissue-like phantom could facilitate optical clearing to be used in quantitative control of tissue optical properties, and further promote the application potential of optical clearing to light-based noninvasive diagnostic and therapeutic techniques.

Keywords: Optical clearing effects; tissue-like phantom; quantitative control; optical properties; scattering effects; optical clearing agents (OCAs).

1. Introduction

Currently, light-based noninvasive diagnostic and imaging techniques have shown a great potential in the field of biomedical photonics, but the strong natural scattering effect of biological tissue limits the depth of light penetration so that it is difficult to obtain more information. In recent years, tissue optical clearing technique proposed by Tuchin *et al.*¹ introduced OCAs such as glycerol,^{2–4} propylene glycol,^{2,5–7} polyethylene glycol,^{8,9} dimethyl sulfoxide (DMSO),^{3,5} oleic acid¹⁰ and borneol¹¹

to medicate on the surface of biological tissues. With the impregnation of OCAs into turbid tissues including skin, muscle, gastric mucosa and sclera, etc., light penetration depth could be enhanced and optical imaging contrast could be improved. One of the current acceptable explanations for optical clearing mechanism is the reduction of light scattering.

Previous studies were performed by using various techniques and methods, for example, Fourier transform infrared spectroscopic imaging,¹² optical

coherence tomography (OCT),^{2,6,13} laser speckle contrast imaging,¹⁴ mass loss assessment,¹⁰ transdermal skin resistance (TSR) measurement³ and second-harmonic generation (SHG) imaging.¹⁵ The existing results are encouraging, since it seems that optical clearing by use of OCAs could enable turbid tissue to become optically clear. Thus more and more researchers have focused their interests on this new method and numerous publications have been published to demonstrate the effects of tissue optical clearing. Up to now, there are three generally accepted views of mechanisms of light scattering reduction by OCAs^{1,16,17}: (1) dehydration of biological tissue constituents; (2) replacement of interstitial or intracellular liquids with an agent that creates a better refractive index matching environment; and (3) structural modification of dissociation of collagen. Besides, other unspecified mechanisms could be working synergistically at the same time.

Despite the fact that optical clearing brings a delightful potential in applications for light-based therapeutic and diagnostic as well as optical imaging techniques, the quantitative correlation between the doses of OCAs penetrating into biological tissue at different time intervals and the scattering reduction of tissues caused by OCAs is still relatively poorly understood. This is mainly because the discrepancies of physiological structures widely exist in different tissues, even in the same section of tissues dissected from different biological individuals. Therefore, the response of tissue diversities leads to great difficulty to understand optical clearing effects quantitatively. To clarify the mechanisms of optical clearing in the reduction of scattering effects in biological tissues, there is a need to perform further systematic studies to delineate the interactions between OCAs and tissues. In this regard, homogeneous tissue-like phantoms, with strong stability and easily tunable optical properties, were introduced to investigate optical clearing effect by the use of OCAs. Various phantoms have widely been applied to optical spectroscopy, imaging¹⁸ and often used to mimic the optical properties of human or animal tissues.

Motivation of this work includes: (1) by using tissue-like phantoms with given optical properties, to present a quantitative connection between the change of optical properties and the dose of OCAs into tissue-like phantoms; (2) to quantify the relation between the penetration depth and the dose of OCAs at different time intervals.

2. Materials and Methods

2.1. Preparation of optical clearing agents

DMSO and glycerol were chosen, in this work, not only because they are common OCAs for optical clearing currently, but also because their functional groups have no molecular interaction¹⁹ with the components of tissue-like phantoms. Anhydrous DMSO and glycerol were purchased from Shanghai Sangon Biological Engineering Technology and Service Co. Ltd., China. In order to investigate the optical clearing effects of different OCAs, the volume fraction (v/v) of OCAs added into every tissue-like phantom was kept constant; similarly, principal components of tissue-like phantoms are kept unchanged.

2.2. Tissue-like phantoms preparation

Tissue-like phantom was first used for breast cancer imaging¹⁸ in the early 1980s. It usually includes matrix materials, absorbing materials and scattering materials. After comprehensive evaluation of the fabricating cost and set-up of laboratory conditions, the following principal components of tissue-like phantom were used in this work: agar powder (A-7049, Sigma, USA) as matrix, India ink (Solarbio Science and Technology Co., Ltd., China) as absorber and intralipid-20% (Sino-Swed Pharmaceutical Corp. Ltd., China) as scattering material. First, agar powder was mixed with 70°C distilled water and heated to the melting temperature of 95°C.²⁰ Then, India ink, intralipid and OCAs were added into the agar mixture at the optimal temperature of 75°C, and the solution was stirred continuously with magnetic stirrer until it cooled down to 50°. Finally, the solution was poured into the mold with a chamber of 80 mm diameter. A few minutes later, a 1-mm thick phantom can be taken out of the mold for investigation. All the samples were prepared by using the same bottle of India ink and 20% intralipid, to ensure that the optical properties of tissue-like phantoms would not generate significant variations.

In this work, 14 groups of tissue-like phantoms were prepared as shown in Table 1. Five identical phantom samples for each group were prepared and measured at different time and the final result for each group was the average value of five measurements.

Table 1. Tissue-like phantoms used in this work, where the percentage of agar represents mass fraction and the others stand for volume fraction in total mixture solution.

| Phantom group | Agar (%) | India ink (%) | Intralipid (%) | Glycerol (%) | DMSO (%) |
|---------------|----------|---------------|----------------|--------------|----------|
| 1 | 1.5 | 1 | 1 | 0 | 0 |
| 2 | 1.5 | 1 | 2 | 0 | 0 |
| 3 | 1.5 | 1 | 3 | 0 | 0 |
| 4 | 1.5 | 1 | 4 | 0 | 0 |
| 5 | 1.5 | 1 | 5 | 0 | 0 |
| 6 | 1.5 | 1 | 6 | 0 | 0 |
| 7 | 1.5 | 1 | 2 | 10 | 0 |
| 8 | 1.5 | 1 | 2 | 20 | 0 |
| 9 | 1.5 | 1 | 2 | 30 | 0 |
| 10 | 1.5 | 1 | 2 | 35 | 0 |
| 11 | 1.5 | 1 | 2 | 0 | 10 |
| 12 | 1.5 | 1 | 2 | 0 | 20 |
| 13 | 1.5 | 1 | 2 | 0 | 30 |
| 14 | 1.5 | 1 | 2 | 0 | 35 |

2.3. Tissue samples preparation

Fresh porcine skin was obtained from an accredited slaughter house with muscle and fat tissue layers removed using a scalpel blade. After depilation, porcine skin was cut as circle pieces with a diameter of 80 mm. The sample pieces were immediately sealed in a plastic bag to prevent them from natural dehydration, and kept frozen in a freezer at -80°C until sectioning. When needed, frozen native skin tissue sections were thawed to 4°C . The average thickness of porcine skin was 1.1 ± 0.04 mm. The samples were left at room temperature for 30 min before each measurement.

2.4. Experiment set-up and analytical methods

A double-integrating-spheres (SPH-12, SphereOptics, USA) system (DIS) (Fig. 1) was constructed for the diffuse reflectance and total transmittance

measurements of tissue-like phantom and skin tissue samples before and after treatment by OCAs. As a light source, a He-Ne laser with a diameter of 1.5 mm was used in the measurement ($\lambda = 632.8$ nm used in this work). The inner diameter of the two spheres is 304.8 mm. The diameters of the entrance port and sample port are 6 mm and 50.8 mm, respectively. The lateral size of the investigated samples must cover the whole area of sample cell. Two Si photodiodes (S2592-04, Hamamatsu Photonics K.K., Japan) were used to collect diffused reflectance (D1) and total transmittance (D2). Data collected by the photodiodes were sent to a computer through a 16-bit data acquisition card (PCI-MIO-16XE-50, National Instrument Inc., USA).

Using inverse adding-doubling (IAD) numerical procedure developed by Prahl *et al.*,^{21,22} we can calculate the absorption (μ_a) and the reduced scattering coefficients ($\mu'_s = \mu_s(1-g)$) of samples. Here μ_s is the scattering coefficient and g is the anisotropy factor of scattering, the value of which is fixed at 0.9 for biological tissues and 0.636 for homemade phantom. If the program did not converge to a unique set of optical property parameters, the results were discarded.

The refractive index of sample is an important parameter because it describes the speed of light in a sample and it governs how the photons migrate.²³ In this work, the refractive index of tissue-like phantoms can be derived from Gladstone–Dale's Law,¹ which demonstrates that the resulting value is responsible for the refractive indices of the components related to their volume fractions.

$$n_{\text{phantom}} = \sum_i^N n_i V_i, \quad \sum_i V_i = 1, \quad (1)$$

where n_i and V_i are the refractive index and volume fraction of each component, respectively. N is the number of components.

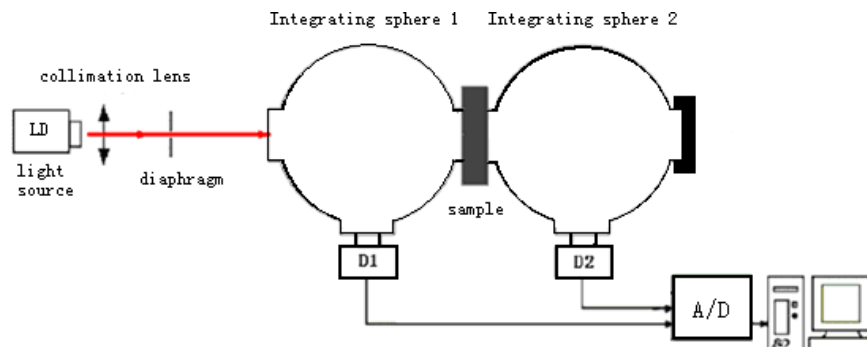


Fig. 1. Schematic of the double-integrating-sphere system.

The refractive index n of porcine skin can be calculated using the following expression²³:

$$n_{\text{skin}} = 0.7(A - B\lambda + C\lambda^2 - D\lambda^3 + E\lambda^4 - f\lambda^5) + 0.3 \times 0.5, \quad (2)$$

where $A = 1.58$, $B = 8.45 \times 10^{-4}$, $C = 1.10 \times 10^{-6}$, $D = 7.19 \times 10^{-10}$, $E = 2.32 \times 10^{-13}$, $F = 2.98 \times 10^{-17}$, and the wavelength λ is in nanometers.

The relative reduction percentage of reduced scattering coefficients (μ'_s) of both skin tissues and tissue-like phantoms was calculated using Eq. (3).⁷ And then it was used to derive the concentration of OCAs penetrating into skin tissues at different time intervals.

$$SRP = \frac{\mu'_{s \text{ treated}} - \mu'_{s \text{ original}}}{\mu'_{s \text{ original}}}, \quad (3)$$

where the subscript “treated” refers to the samples medicated with OCAs at different time intervals for skin tissues and different concentrations for tissue-like phantoms; “original” represents the samples treated without OCAs.

3. Results

3.1. Optical properties of tissue-like phantom

The optical stabilities of tissue-like phantoms were checked by calculating MSE (Mean Square Error) of absorption coefficient (MSE < 0.5%) and scattering coefficient (MSE < 5.95%). The results showed that homemade tissue-like phantoms are stable enough to be used for the following experiments.

It can be seen from Fig. 2 that there is a linear relationship between reduced scattering coefficients

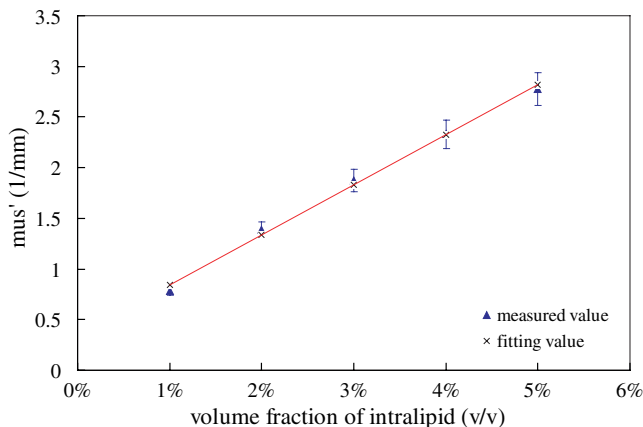


Fig. 2. Reduced scattering coefficient of tissue-like phantoms with different concentration of intralipid.

(μ'_s) and the different concentrations of intralipid [IL in Eq. (4)].

This relationship could be fitted as Eq. (4) without considering the influence of the agar.

$$\mu'_s{}^{\text{phantom}} = 49.418 \cdot C_{IL} + 0.3499. \quad (4)$$

In the same way, the relationship between absorption coefficients of tissue-like phantoms and India ink (ink in equation) and intralipid (IL in equation) is shown by Eq. (5).

$$\mu'_a{}^{\text{phantom}} = 8.602 \cdot C_{\text{ink}} + 0.7544 \cdot C_{IL} - 0.0058. \quad (5)$$

3.2. Optical clearing effect of tissue-like phantom

Since the optical properties can be easily tuned in a well-controlled way, tissue-like phantoms with absorption and reduced coefficients in accordance with biological tissues²⁴ can be prepared for the study of optical clearing effect. In this work, we selected India ink with concentration of 1% and intralipid with 2% to mimic optical properties of human skin tissue. And to determine how the OCAs affect the absorption and scattering coefficients of tissue-like phantom, 1-mm-thick sections with different OCA concentrations (sample-6 to sample-14) were prepared. Diffuse reflectance and total transmittance were measured by using DIS at 632.8 nm, and the absorption and reduced scattering coefficients were then calculated by IAD arithmetic.

Figure 3 demonstrated the optical clearing effects of tissue-like phantoms with different concentrations of OCAs. Both glycerol and DMSO can reduce the scattering effect of tissue-like phantoms; moreover, the reduced scattering coefficient decreased almost linearly with the variation of the concentration of OCAs from 0% to 35%. According to the results represented, we can conclude that the formulas [Eqs. (6) and (7)] quantitatively describe the relationship between the reduced scattering coefficient of phantoms and the concentration of OCAs.

$$\mu'_S{}^{\text{GLY}} = 49.418 \cdot C_{IL} - 2.319 \cdot C_{\text{GLY}} + 0.3091. \quad (6)$$

$$\mu'_S{}^{\text{DMSO}} = 49.418 \cdot C_{IL} - 2.8868 \cdot C_{\text{DMSO}} + 0.3996. \quad (7)$$

Since glycerol and DMSO have no strong absorbing bands with the range of 400–840 nm,¹

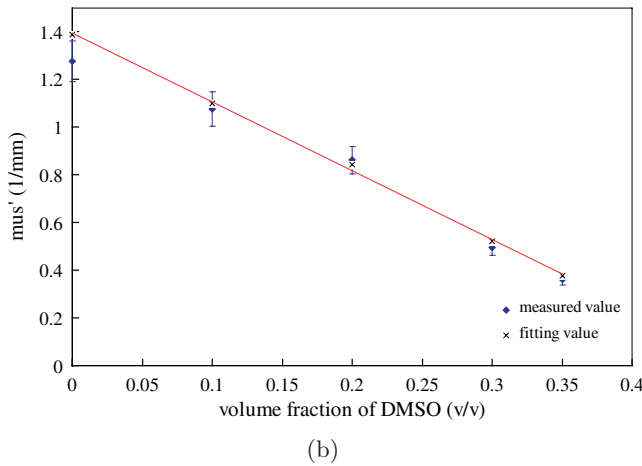
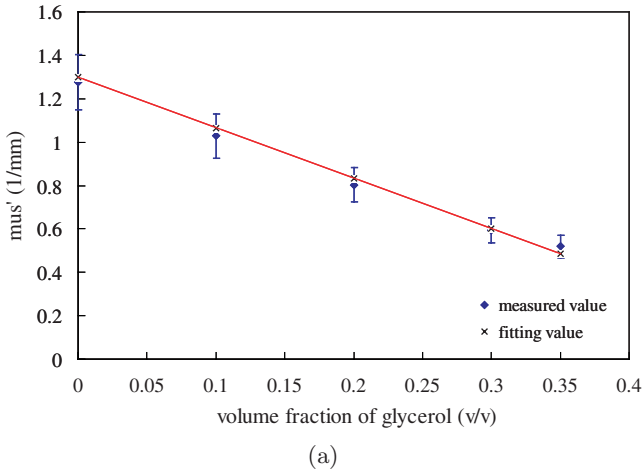


Fig. 3. Optical clearing effect induced by OCAs with different concentrations. (a) Reduction of scattering effect of tissue-like phantoms with different doses of glycerol. (b) Reduction of scattering effect of tissue-like phantoms with different doses of DMSO.

Eq. (5) could still be used to describe the absorption of tissue-like phantoms even after mixing with different concentration of OCAs.

The depth of light penetration into a tissue-like phantom is an important parameter for evaluation of the optical clearing effect by OCAs. It can be calculated by Eq. (8)^{25,26}:

$$\delta = \frac{1}{\sqrt{3\mu_a(\mu_a + \mu'_s)}}. \quad (8)$$

It can be concluded from Fig. 4 that the higher the concentration of OCAs mixing in tissue-like phantom, the deeper the depth of light penetration into it. The value is correspondingly equal to 1.63, 1.82, 2.07, 2.58, and 2.97 mm for DMSO, as well as 1.61, 1.65, 1.97, 2.25, and 2.4 mm for glycerol. It can also be seen that the optical penetration depth of DMSO is larger than that of glycerol, which proved

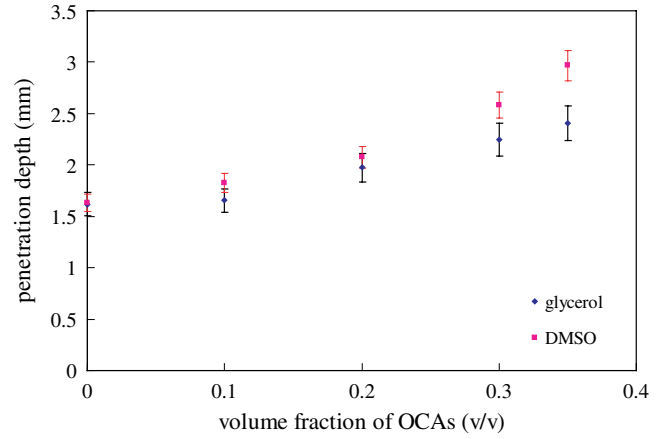


Fig. 4. Optical penetration depth δ of light into tissue-like phantom over the concentration range from 0% to 35%.

that DMSO has a better optical clearing effect than glycerol as shown elsewhere.

3.3. Scattering reduction of porcine skin applied with glycerol and DMSO

Figure 5 shows the changes of reduced scattering coefficients of porcine skin tissue medicated with glycerol and DMSO solutions respectively at different time intervals. It can be seen that μ'_s of porcine skin decreased gradually over the time course after OCAs were medicated on the surface of skin tissues. And it becomes flat after 40 min, probably because the dose of OCAs in skin tissues became almost saturated and a better refractive index matching environment could be created.

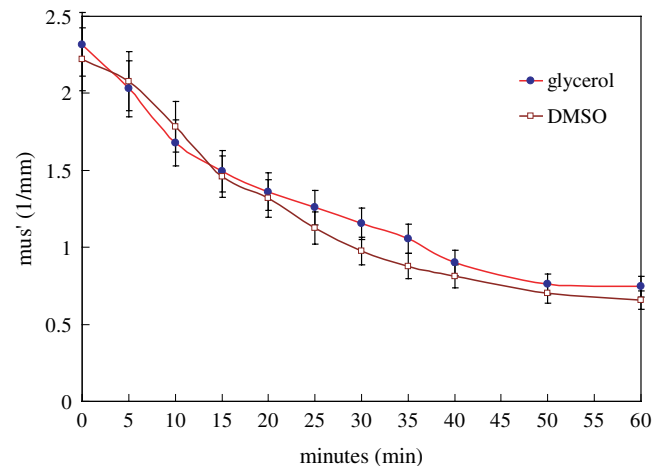


Fig. 5. Reduced scattering coefficients of porcine skin tissue after 0, 5th, 10th, 15th, 20th, 25th, 30th, 35th, 40th, 50th and 60th-min treatment by glycerol and DMSO, respectively.

4. Discussion

Tissue optical clearing technique, which has the ability to help light penetrate deeper within biological tissues, plays an essential role in the field of biomedical photonics, especially in enhancing the capabilities of noninvasive or minimally invasive light-based diagnostic and imaging techniques. Although numerous studies have demonstrated that the optical clearing would reduce scattering effects and improve the imaging contrast of biological tissues,^{27–29} reports of quantitative analysis to evaluate the correlation between the dose of OCAs and the changes of optical properties of biological tissue treated with OCAs are still uncommon. The reason is that biological tissues may present different optical properties within visible and near-infrared range, even the same anatomic site of tissues. In this work, to quantitatively study the optical clearing effects by the use of OCAs such as glycerol and DMSO, tissue-like phantoms were introduced to mimic the optical characteristic of biological tissues. The optical properties of phantoms can be easily controlled by adjusting the ratio between absorbers and scatterers consisted in phantoms. By adding a certain amount of OCAs into tissue-like phantoms to replace part of distilled water under the condition of the constancy of total volume, the optical clearing effect of tissue-like phantoms was studied. Moreover, the quantitative correlation between the reduction of scattering effect and the dose of OCAs was presented. The results have demonstrated that the scattering coefficients decreased almost linearly with the increase of glycerol and DMSO, respectively. Take glycerol as an example. The reduced scattering coefficient was decreased by 12.85%, 36.99%, 53.44% and 59.21% when 10%, 20%, 30%, and 35% glycerol concentrations (v/v) were used compared with that of original phantom.

The optical penetration depth, a significant parameter, is the main limitation in most state-of-the-art optical approaches, for example, OCT imaging or noninvasive optical blood glucose sensing. It can be concluded from Fig. 4 that the light penetration depth into the phantoms is increased, with the maximum depth percentage reaching 48.76% with glycerol and 81.65% with DMSO, proving that tissue-like phantoms become optically cleared and OCAs could reduce the highly scattering effect of phantoms effectively.

Since the structure of porcine skin is quite similar to human skin, porcine skin has been selected in this work for *in vitro* experiments. As shown in Fig. 5, we calculate the reduced scattering coefficient of porcine skin before and after the immersion of OCAs at 0, 5th, 10th, 15th, 20th, 25th, 30th, 35th, 40th, 50th and 60th min. It can be concluded that the optical clearing effects caused by DMSO were better than that of glycerol. To compare the optical clearing effects with tissue-like phantoms, here we calculated the reduction percentage caused by glycerol only, which is 12.34%, 27.54%, 35.52%, 41.30%, 45.66%, 50.24%, 54.51%, 61.20%, 61.20%, 67.20%, and 67.85% as time increases. Therefore, we can conclude the quantitative correlation between the dose of glycerol penetrating into biological tissue and the reduction of scattering effect induced by glycerol, i.e., the concentration penetrating into porcine skin at 5-min interval is about 5%, and at 35-min interval is about 30%.

The multilayer structure (stratum corneum, viable epidermis and dermis) and anisotropic physical property of skin tissue limit the penetration depth of light due to the highly scattering effect, which results from the refractive index mismatch between intercellular fluids and cell organelles and fibers. Optical clearing approach by the use of OCAs with higher refractive index of around 1.47, could reduce the scattering effect by giving rise to a better refractive index match, which could greatly improve the applications of light-based therapeutic and diagnostic techniques, as well as optical imaging techniques. When OCAs diffuse into skin tissue, they could replace some intercellular fluid of skin tissue, causing an increase in the refractive index of the fluid; therefore, the reduced scattering coefficient decreases (similar results to Ref. 19), leading to an increase in light penetration depth. Experimental results suggested that the mechanism of optical clearing effect of tissue-like phantom mixing with different concentration of OCAs is the same as that stated in Sec. 1.

5. Conclusion

In this work, we have shown that optical properties of tissue-like phantoms can be easily controlled and tuned based on our fitting formulas. Furthermore, by use of tissue-like phantoms, we investigated the correlation between the reduction of scattering effect and dose of OCAs penetrating into

biological tissue. In conclusion, tissue-like phantom should be a good tool for investigating the effects of tissue optical clearing.

Acknowledgments

This work was supported by the National Natural Science Foundation of China (NSFC, Nos. 30600126, 30700168 and 30900275).

References

1. V. V. Tuchin, I. L. Maksimova, D. A. Zimnyakov, I. L. Kon, A. H. Mavlutov, A. A. Mishin, "Light propagation in tissues with controlled optical properties," *J. Biomed. Opt.* **2**, 401–407 (1997).
2. V. V. Tuchin, X. Xu, R. K. Wang, "Dynamic optical coherence tomography in optical clearing, sedimentation and aggregation study of immersed blood," *Appl. Opt.* **41**, 258–271 (2002).
3. J. Jiang, R. K. Wang, "Comparing synergistic effects of oleic acid and dimethyl sulfoxide as vehicle on optical clearing of skin tissue *in vitro*," *Phys. Med. Biol.* **49**, 5283–5294 (2004).
4. S. Plotnikov, V. Juneja, A. B. Isaacson, W. A. Mohler, P. J. Campagnola, "Optical clearing for improved contrast in second harmonic generation imaging of skeletal muscle," *Biophys. J.* **90**, 328–339 (2006).
5. J. Jiang, R. K. Wang, "Synergistic effect of hyperosmotic agents under topical application on optical clearing of skin tissue *in vitro*," *Proc. SPIE* **5696**, 80–90 (2005).
6. R. K. Wang, X. Xu, V. V. Tuchin, J. B. Elder, "Concurrent enhancement of imaging depth and contrast for optical coherence tomography by hyperosmotic agents," *J. Opt. Soc. Am. B* **18**, 948–953 (2001).
7. Z. Zhi, Z. Han, Q. Luo, *et al.*, "Improve optical clearing of skin *in vitro* with propylene glycol as a penetration enhancer," *J. Innovat. Opt. Health Sci.* **2**(3), 269–278 (2009).
8. A. Matsui, S. J. Lomnes, J. V. Frangioni, "Optical clearing of the skin for near-infrared fluorescence image-guided surgery," *J. Biomed. Opt.* **14**(2), 024019 (2009).
9. Z. Mao, D. Zhu, Y. Hu, *et al.*, "Influence of alcohols on the optical clearing effect of skin *in vitro*," *J. Biomed. Opt.* **13**(2), 021104 (2008).
10. R. K. Wang, J. B. Elder, "Propylene glycerol as a contrasting agent for optical coherence tomography to image gastro-intestinal tissues," *Laser Surg. Med.* **30**, 201–208 (2002).
11. J. Jiang, W. Chen, K. Xu, R. K. Wang, "Potential application of Chinese traditional medicine (CTM) as enhancer for tissue optical clearing," *Proc. SPIE* **7176**, 71760K1-8 (2009).
12. J. Jiang, M. Boese, P. Turner, R. K. Wang, "Penetration kinetics of dimethyl sulphoxide and glycerol in dynamic optical clearing of porcine skin tissue *in vitro* studied by Fourier transform infrared spectroscopic imaging," *J. Biomed. Opt.* **13**(2), 21101–21105 (2008).
13. H. Liu, B. Beauvoit, M. Kimura, B. Chance, "Dependence of tissue optical properties on solute-induced changes in refractive index and osmolarity," *J. Biomed. Opt.* **1**, 200–211 (1996).
14. D. Zhu, J. Wang, Z. Zhi, *et al.*, "Imaging dermal blood flow through the intact rat skin with an optical clearing method," *J. Biomed. Opt.* **15**(2), 026008 (2010).
15. X. Wen, Z. Mao, Z. Han, V. V. Tuchin, D. Zhu, "In vivo skin optical clearing by glycerol solutions: Mechanism," *J. Biophotonics* **3**, 44–52 (2010).
16. C. G. Rylander, O. F. Stumpp, T. E. Milner, *et al.*, "Dehydration mechanism of optical clearing in tissue," *J. Biomed. Opt.* **11**(4), 041117 (2006).
17. A. T. Yeh, B. Choi, J. S. Nelson, B. J. Tromberg, "Reversible dissociation of collagen in tissues," *J. Invest. Dermatol.* **121**(6), 1332–1335 (2003).
18. B. W. Pogue, M. S. Patterson, "Review of tissue simulation phantoms for optical spectroscopy, imaging and dosimetry," *J. Biomed. Opt.* **11**(4), 0411021-16 (2006).
19. X. Wen, V. V. Tuchin, Q. Luo, *et al.*, "Controlling the scattering of intralipid by using optical clearing agents," *Phys. Med. Biol.* **54**, 6917–6930 (2009).
20. R. Cubeddu, A. Pifferi, P. Taroni, A. Torricelli, G. Valentini, "A solid tissue phantom for photon migration studies," *Phys. Med. Biol.* **42**, 1971–1979 (1997).
21. S. A. Prahl, M. J. C. van Gemert, A. J. Welch, "Determining the optical properties of turbid media by using the adding-doubling method," *Appl. Opt.* **32**, 559–568 (1993).
22. <http://omlc.ogi.edu/software/iad/index.html>.
23. T. L. Troy, S. N. Thennadil, "Optical properties of human skin in the near infrared wavelength range of 1000 to 2200 nm," *J. Biomed. Opt.* **6**(2), 167–176 (2001).
24. V. V. Tuchin, "Tissue optics: Light scattering methods and instruments for medical diagnosis," *SPIE Press*, Washington, USA (2000).
25. A. N. Bashkatov, E. A. Genina, V. I. Kochubey, V. V. Tuchin, "Optical properties of human skin, subcutaneous and mucous tissues in the wavelength range from 400 to 2000 nm," *J. Phys. D: Appl. Phys.* **38**, 2543–2555 (2005).
26. C. Liu, Z. Zhi, V. V. Tuchin, *et al.*, "Enhancement of skin optical clearing efficacy using photo-irradiation," *Lasers Surg. Med.* **42**, 132–140 (2010).

27. X. Xu, R. K. Wang, J. B. Elder, V. V. Tuchin, "Effect of dextran-induced changes in refractive index and aggregation on optical properties of whole blood," *Phys. Med. Biol.* **48**, 1205–1221 (2003).
28. G. Vargas, E. K. Chan, J. K. Barton, H. G. Rylander, A. J. Welch, "Use of an agent to reduce scattering in skin," *Lasers Surg. Med.* **24**, 133–144 (1999).
29. Y. He, R. K. Wang, "Dynamic optical clearing effect of tissue impregnated with hyperosmotic agents and studied with optical coherence tomography," *J. Biomed. Opt.* **9**(1), 200–206 (2004).